

## SUPPORTING INFORMATION

# A single-molecule FRET sensor for monitoring DNA synthesis in real time

Carel Fijen, Alejandro Montón Silva, Alejandro Hochkoeppler and Johannes Hohlbein

### Alternating-laser excitation (ALEX)

Alternating-laser excitation (ALEX) is a technique in which both donor and acceptor dyes are excited in an alternating fashion.<sup>38,39</sup> In addition to  $f_{D_{exc}}^{D_{em}}$  and  $f_{D_{exc}}^{A_{em}}$  detected in standard smFRET experiments, the ALEX scheme also monitors the acceptor emission after acceptor excitation  $f_{A_{exc}}^{A_{em}}$  allowing to separate donor-only and acceptor-only species from molecules that have both a donor and acceptor. The value in use to identify these species is called the stoichiometry ratio  $S$ :

$$S^{\text{raw}} = \left( f_{D_{exc}}^{A_{em}} + f_{D_{exc}}^{D_{em}} \right) / \left( f_{D_{exc}}^{A_{em}} + f_{D_{exc}}^{D_{em}} + f_{A_{exc}}^{A_{em}} \right)$$

A second advantage of using ALEX is the easy application of correction factors to calculate accurate FRET efficiency  $E$  from apparent FRET efficiency  $E^*$ .

Calculating intramolecular distances using accurate FRET

The FRET efficiency  $E$  describes a distance-dependent energy transfer according to

$$E = \frac{1}{1 + (R/R_0)^6}$$

in which  $R$  is the inter dye distance and  $R_0$  is the Förster radius.  $R_0$  depends on the dye pair in use and corresponds to the distance at which  $E$  equals 0.50. To obtain  $E$ , the apparent FRET efficiency  $E^*$  is corrected for direct excitation of the acceptor, leakage of the donor into the acceptor channel and the gamma factor, which is a measure for the detection efficiencies of the dyes and their quantum yields.<sup>38,40</sup> Correction factors for leakage and direct excitation can be deduced from the peaks of donor-only and acceptor-only species, respectively. A third correction needs to be done for the effect of the quantum yields and detection efficiencies of the dyes, which is represented by the gamma factor. The value of gamma is determined by comparing the stoichiometries of populations at different FRET efficiencies: a value of gamma other than 1, will cause these stoichiometries to be different. In practice, gamma can be calculated from the slope when plotting  $1/S$  against  $E$ .<sup>40</sup> For the distance determination of the polymerized sensors, we used  $R_0 = 6.2$  nm.<sup>44</sup>

## Step by step guide for Hidden Markov Modelling (HMM) analysis using ebFRET

- 1) Hand selected time traces that indicated one or more polymerization events were loaded into ebFRET.
- 2) The selected time traces are filtered for photo bleaching: Parts that indicated a bleached acceptor were excluded from further analysis.
- 3) Due to the long duration of measurements, some traces were partially effected by focus drift. We therefore decided to exclude these parts, in which no polymerisation reaction was visible, from further analysis.
- 4) The priors needed for HMM were taken from the  $E^*$  values of the non-polymerised and the fully polymerised DNA sensor, respectively.
- 5) Before running ebFRET, the ideal number of states (related to the number of steps in the polymerization reaction) is unknown. Fitting was therefore performed successively for two to six states. Even within a single experiment, the noise level can be different between single traces. Therefore, care should be taken not to overestimate the number of present states especially within noisy traces. After running ebFRET for a respective number of states, all traces were manually inspected for cases of over- or underestimation of the number of present states and excluded from further analysis when required.
- 6) For the +25/-7 sensor, the start time of DNA synthesis  $t_1$  was determined using ebFRET as the time point between the initial state and the second fitted state. In the case of the +12/-12 sensor, we decided to pick the highest  $E^*$  value as the starting time  $t_1$  just before polymerization as ebFRET was not reliably able to pick up these characteristic short peaks in  $E^*$ .
- 7) In cases with two low final  $E^*$  values present in a time trace, the lowest one was chosen to determine the polymerization time  $t_2$ . The main consideration here is that there is not one specific FRET efficiency value that corresponds to a polymerized construct. Rather, the FRET efficiencies of polymerized molecules appear to be normally distributed around a mean value of  $E^* \approx 0.18$  (for the +25/-7 sensor). We looked at the widths of the Gaussian fits in Figure 2, and decided to set the cut-off value at 0.25. This corresponds to the mean value plus approximately one standard deviation.

### Polymerization at the ensemble level monitored in a plate reader

The polymerization of the +25/-7 sensor by KF was recorded in a 96 wells plate, using a SpectraMax M2 plate reader. dNTPs (100  $\mu$ M each) and sensors (10 pmoles, to reach a concentration of 100 nM) were mixed together in an aliquot resembling our imaging buffer, but without the oxygen scavenger system. An emission spectrum (excitation at 500 nm) was taken before addition of polymerases (see Fig. S6a, dotted line). By exciting at 500 nm instead of 560 nm, the excitation efficiency is decreased by a factor of  $\sim 3$ . After mixing polymerases (20 nM) into the buffer to create a total reaction volume of

100  $\mu$ L, emission intensities at 575 and 665 nm were recorded for 600 s (Fig. S6b). Immediately after this recording, another emission spectrum was taken (Fig. S6a, solid line).

### **Denaturing PAGE gel to assess influence of fluorescent labels on polymerase speed**

We performed a series of bulk primer-extension polymerizations on our +25/-7 sensor, our +12/-12 sensor and on an unlabelled version of the same construct. DNA (final concentration: 25 nM) and KF (final concentration: 100 nM) were mixed together in a buffer similar to our imaging buffer, but without the oxygen scavenger system. A fraction of this solution was taken as measurement  $t = 0$  s. Addition of dNTPs (final concentration: 500 nM each) started the reactions. Reactions were quenched with EDTA after 15 s, 30 s, 60 s, 120 s and 300 s. Because reaction speed of DNA synthesis is too fast at room temperature, we performed the reactions in a cold room at 6 °C. This temperature does not considerably change the  $K_d$  of KF for primer-template DNA,<sup>50</sup> but it does slow down the polymerization reaction.<sup>51</sup>

Products were mixed with formamide (to 50% v/v), heated for 5 minutes at 95 °C unless otherwise indicated and loaded onto a denaturing PAGE (20%, 6 M urea). After running the gel, DNA bands were visualized using SYBR Gold stain (Fig. S8+9).

Upon inspection of the band pattern, it became clear that the primer is invisible at the concentrations that were used for the assay. Some other constructs were also difficult to detect, probably because of a quenching mechanism between SYBR Gold and Cy3B/ATTO647N. Additionally, unexpected bands running slightly slower than the template were visible. We hypothesized that these bands correspond to non-denatured sensors. To test this hypothesis, we used a few native and fully polymerized sensors that we did not subject to the aforementioned heat treatment. The gel shows that this heat treatment does not always have the desired effect (Fig. S8), leading to the conclusion that non-denatured fractions indeed cause the unexpected bands. Moreover, we noted that fully polymerized sensors are harder to denature than native sensors. We used this principle to identify the progress of polymerization at each time point. To this aim, we measured the increasing intensities of the upper bands (corresponding to fully polymerized product) over time and fitted them to Michaelis-Menten kinetics to extract reaction half-time  $t_{1/2}$  (Fig. S9). We conclude from our data that the rates of polymerisation are comparable between the labelled and unlabelled constructs, but we note that further investigation and, ideally, the use of stopped flow equipment and radioisotope labelled DNA would be required to evaluate the DNA sensors further.

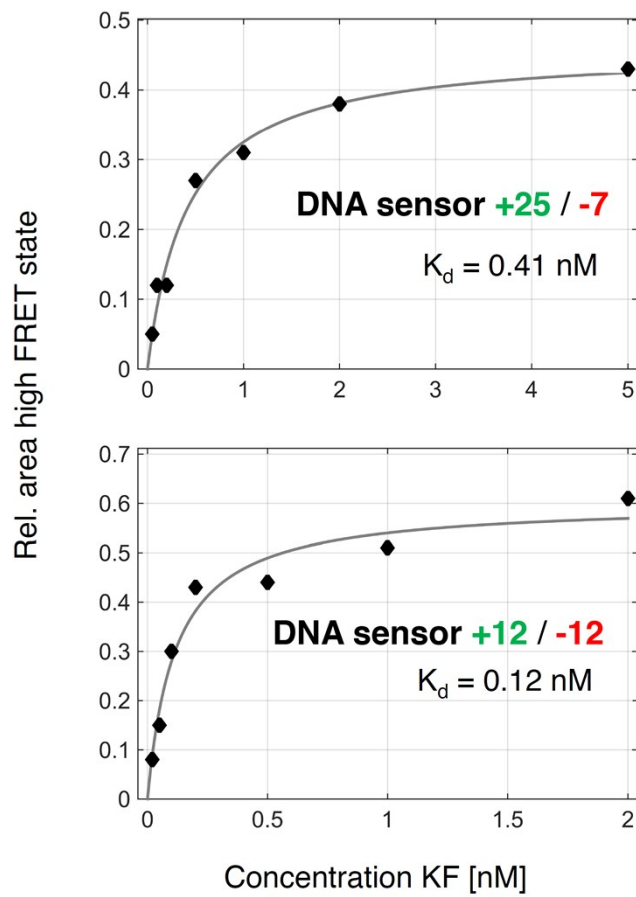


**Figure S1** Binding of KF to the sensors reveals a dissociation constant  $K_d$  of 0.41 nM for the +25/-7 sensor, and a  $K_d$  of 0.12 nM for the +12/-12 sensor (data fitted to Michaelis-Menten kinetics: rel. area high FRET state = (maximum occupancy \* [KF])/([KF] +  $K_d$ )).

Examples KF polymerizing sensor +25/-7

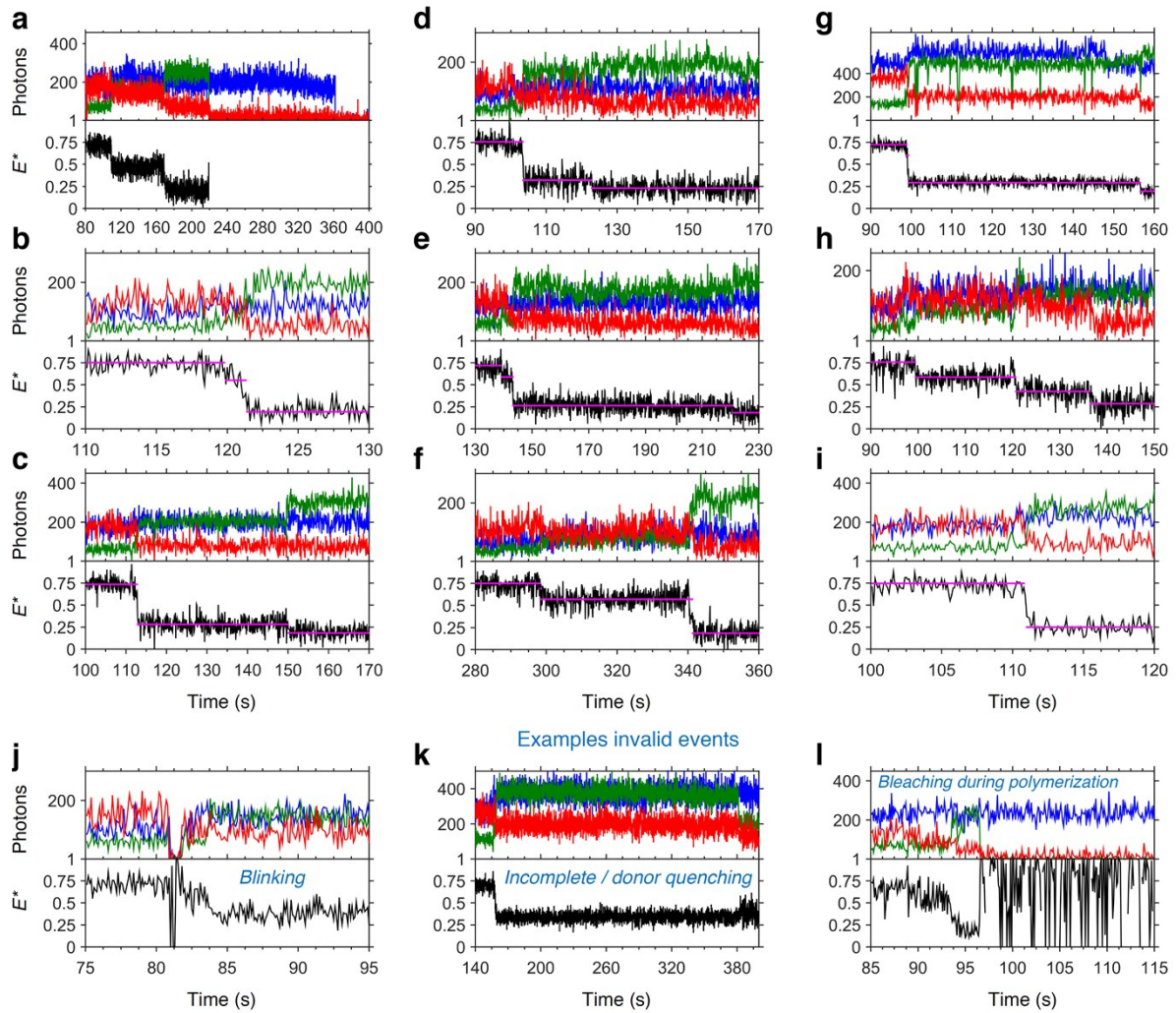


**Figure S2** (a-l) Examples of time traces showing polymerization of the +25/-7 sensor by KF, including a trace showing donor and acceptor bleaching (a). These data were obtained during the same experiment as the trace in Fig. 4a. A few examples of invalid events are shown as well. Events are considered invalid if it is impossible to accurately determine the polymerization time because of either dye blinking (j) or incomplete polymerization ( $E^*_{\text{final}} > 0.3$ ) (k) or quenching or bleaching during a polymerisation event (k, l). Upper panel: Acceptor fluorescence upon direct acceptor excitation (AA; blue trace). Donor (DD, green trace) and acceptor (DA, red trace) fluorescence upon donor excitation. Lower panel: FRET efficiency  $E^*$  (black trace) with fitted HMM model (magenta trace).

Examples POLIII $\alpha$  polymerizing sensor +25/-7

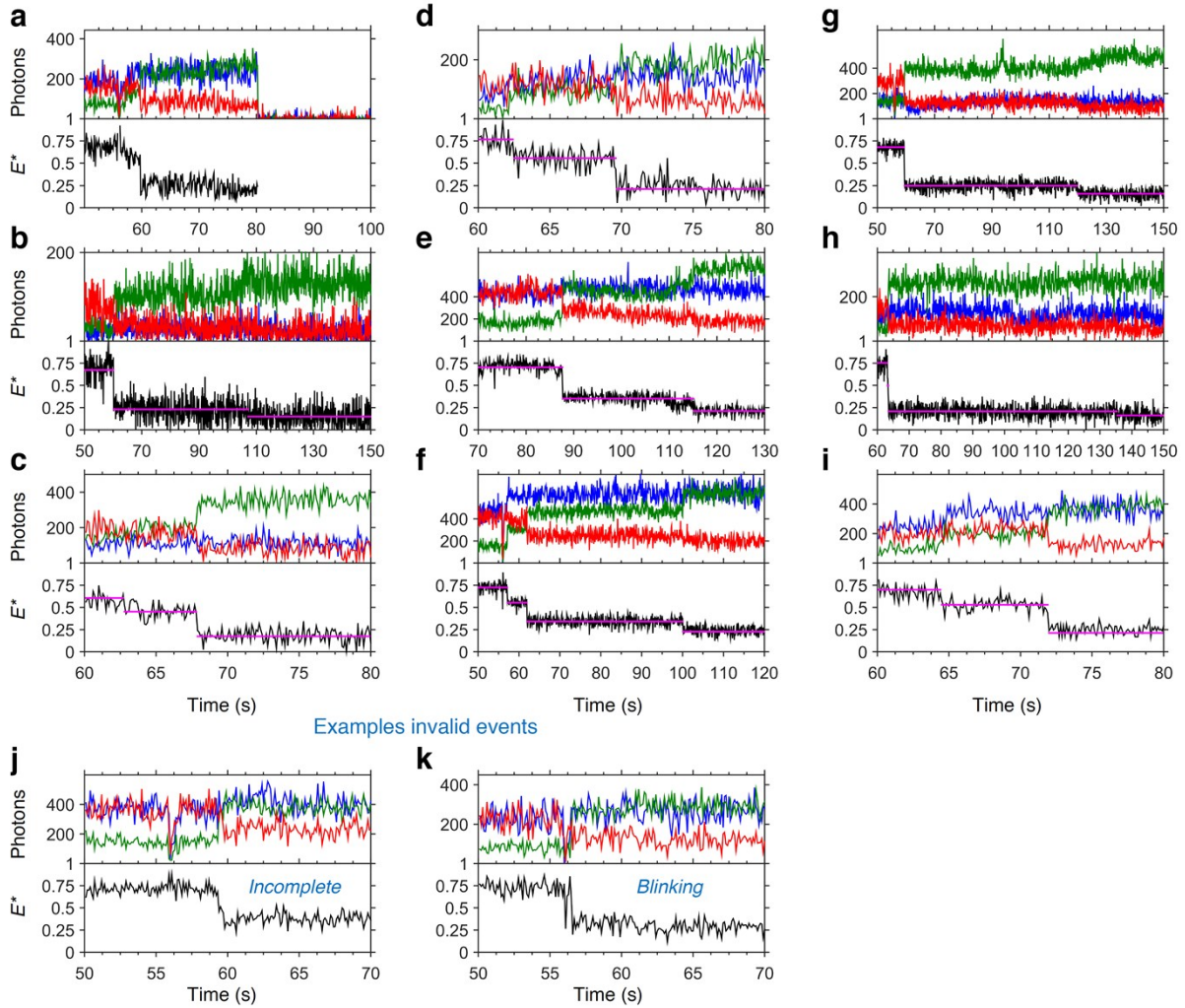


**Figure S3** (a-k) Examples of time traces showing polymerization of the +25/-7 sensor by PolIII $\alpha$ , including a trace showing donor and acceptor bleaching (a). These data were obtained during the same experiment as the trace in Fig. 4b. Examples of invalid events are shown as well. Events are considered invalid if it is impossible to accurately determine the polymerization time because of an incomplete reaction (j) or dye blinking (k). Upper panel: Acceptor fluorescence upon direct acceptor excitation (AA; blue trace). Donor (DD, green trace) and acceptor (DA, red trace) fluorescence upon donor excitation. Lower panel: FRET efficiency  $E^*$  (black trace) with fitted HMM model (magenta trace).

Examples POLB polymerizing sensor +25/-7

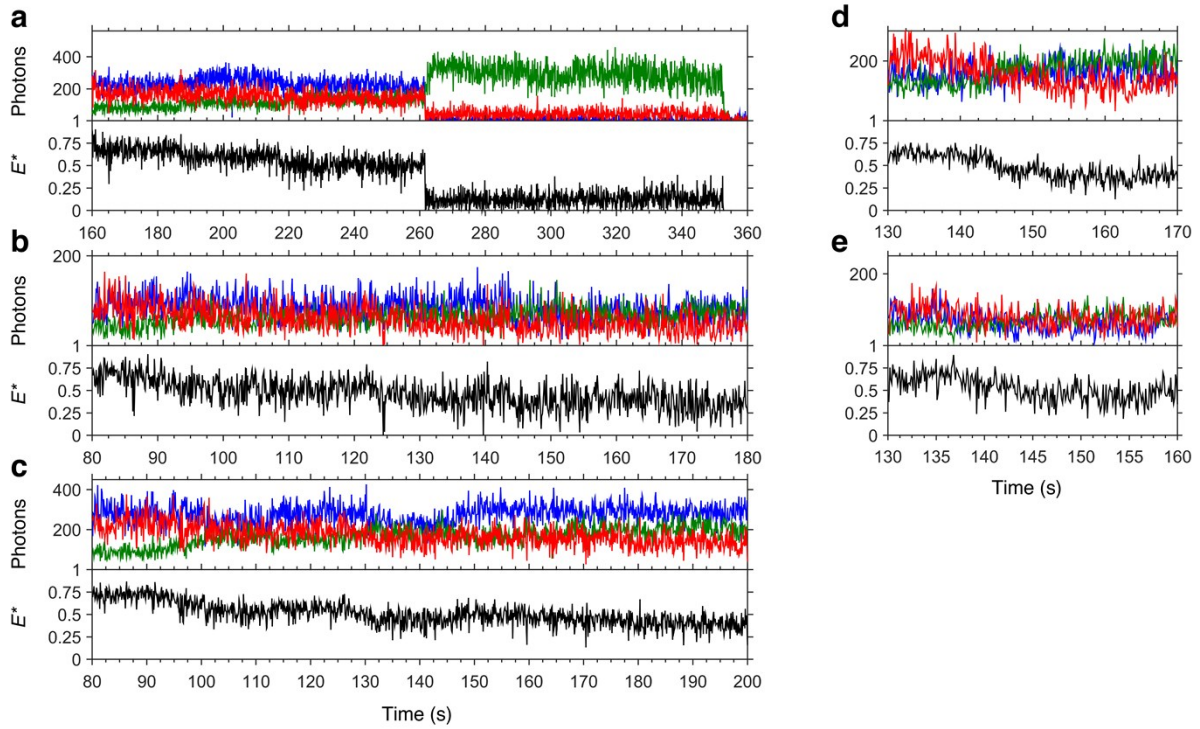


**Figure S4** (a-e) Examples of time traces showing polymerization of the +25/-7 sensor by PolB, including a trace showing donor and acceptor bleaching (a). These data were obtained during the same experiment as the trace in Fig. 4c. Upper panel: Acceptor fluorescence upon direct acceptor excitation (AA; blue trace). Donor (DD, green trace) and acceptor (DA, red trace) fluorescence upon donor excitation. Lower panel: FRET efficiency  $E^*$  (black trace).

Examples KF polymerizing sensor +12/-12

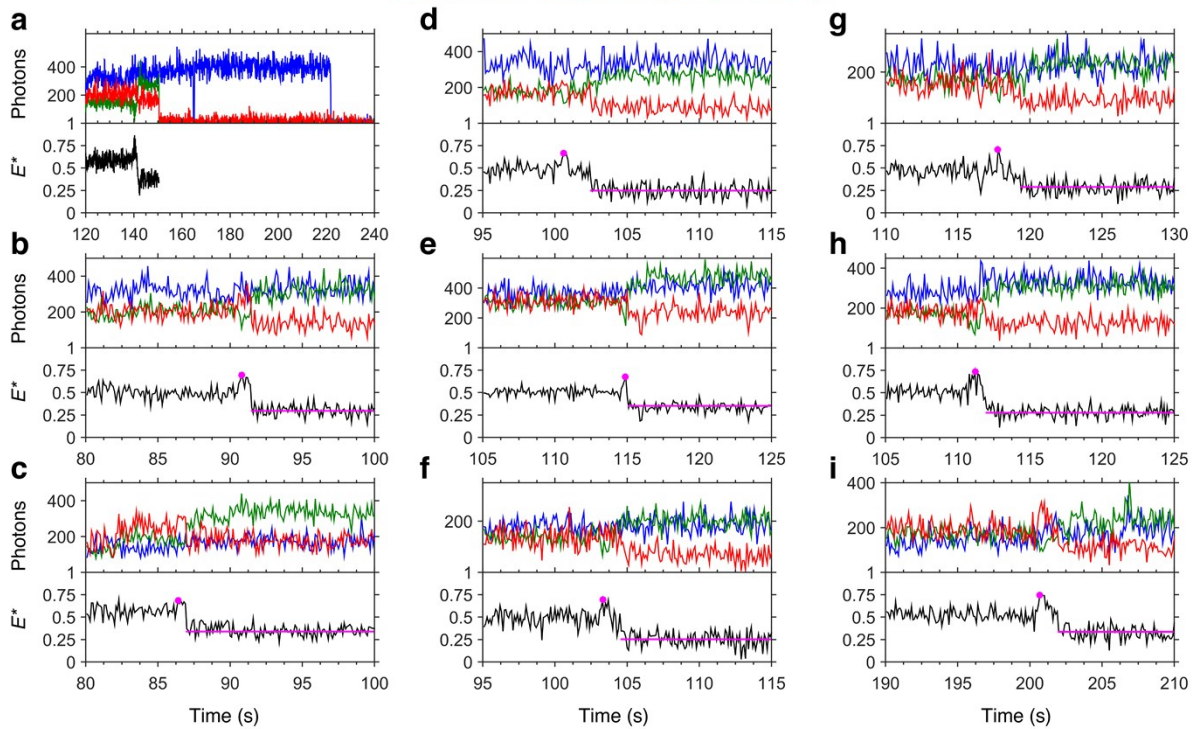


**Figure S5** (a-i) Examples of time traces showing polymerization of the +12/-12 sensor by KF, including a trace showing donor and acceptor bleaching (a). These data were obtained during the same experiment as the traces in Fig. 4g+h. Upper panel: Acceptor fluorescence upon direct acceptor excitation (AA; blue trace). Donor (DD, green trace) and acceptor (DA, red trace) fluorescence upon donor excitation. Lower panel: FRET efficiency  $E^*$  (black trace) with fitted HMM model (magenta trace).



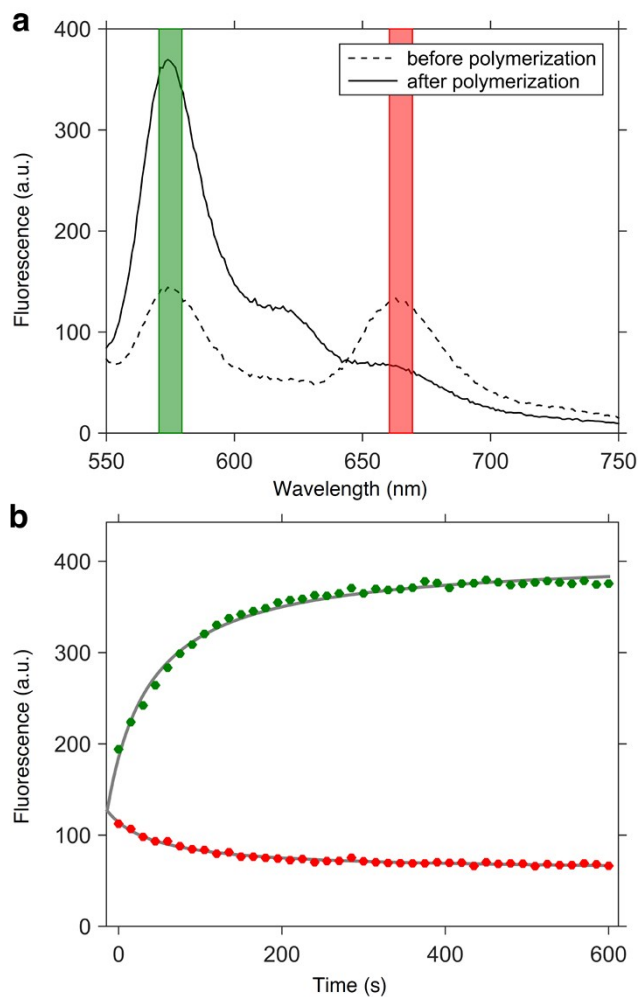


**Figure S6** Polymerization of the +25/-7 sensor by KF, measured in a well plate reader. The emission spectrum recorded before addition of KF shows peaks from emission of Cy3B and ATTO647N (a). The other emission spectrum, taken ~ 600 s after initiation of the reaction, shows an increase in Cy3B fluorescence intensity and a decrease in FRET. Green and red lines indicate the detection wavelengths during the kinetic measurements: 575 nm and 660 nm. Fluorescence intensity followed over time after addition of KF (b) Data fitted to Michaelis-Menten kinetics:

Donor intensity  $I = I_{\max} * (\text{time} + \text{horizontal offset}) / (\text{halftime} + \text{time} + \text{horizontal offset}) + \text{vertical offset}$

Acceptor intensity  $I = - I_{\max} * (\text{time} + \text{horizontal offset}) / (\text{halftime} + \text{time} + \text{horizontal offset}) + \text{vertical offset}$

This fitting shows that the reaction was 50% finished at  $t = 60$  s.

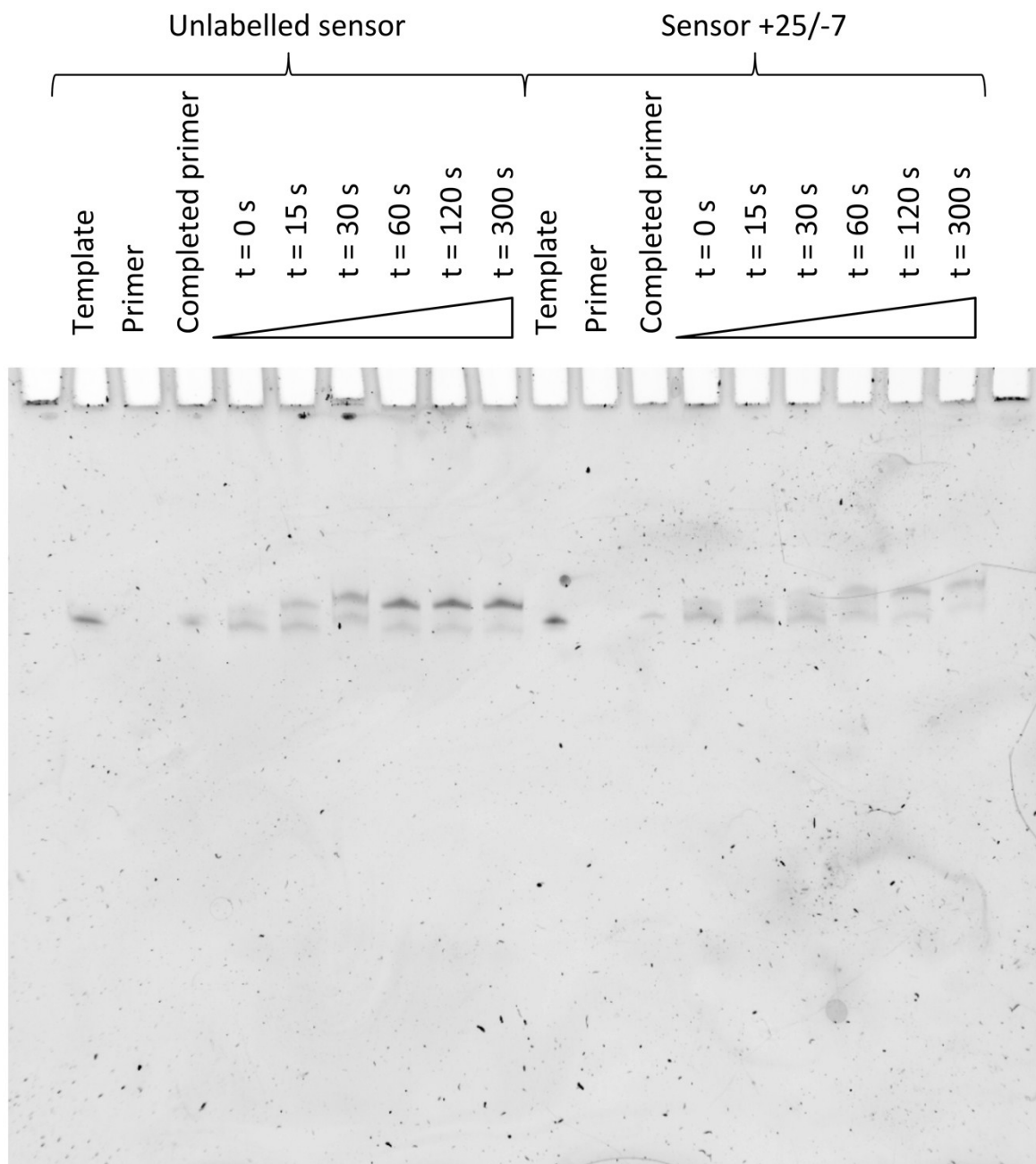


**Figure S7** Polymerization reaction rates were determined from band intensities in denaturing polyacrylamide gels. Gel images show bands corresponding to denatured and non-denatured polymerization products. The increasing intensities of the bands corresponding to fully polymerized product were measured and taken as an indicator for the progress of the reaction.

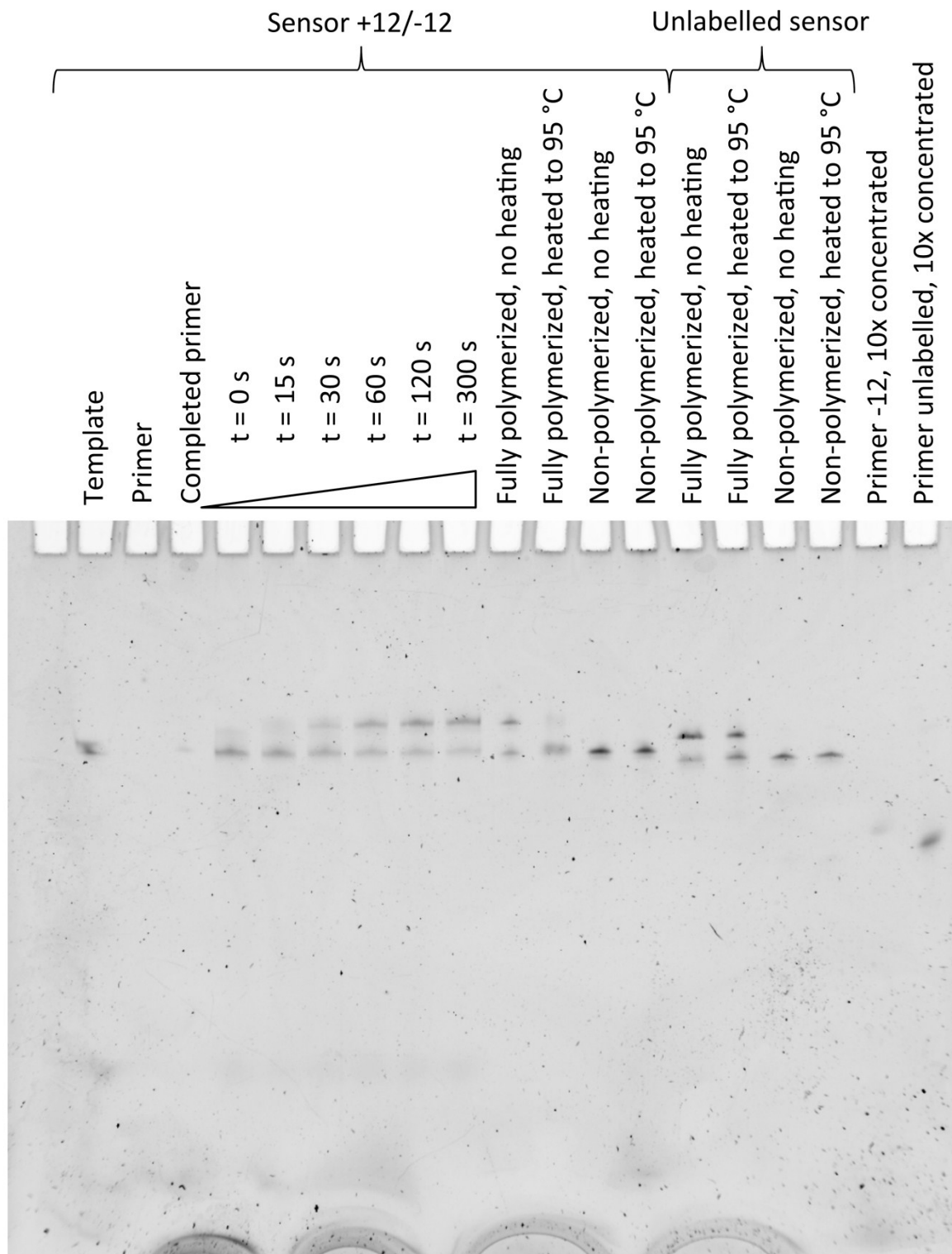


**Figure S8** Polymerization reaction rates were determined from band intensities in denaturing polyacrylamide gels. Gel images show bands corresponding to denatured and non-denatured polymerization products. The increasing intensities of the bands corresponding to fully polymerized product were measured and taken as an indicator for the progress of the reaction.

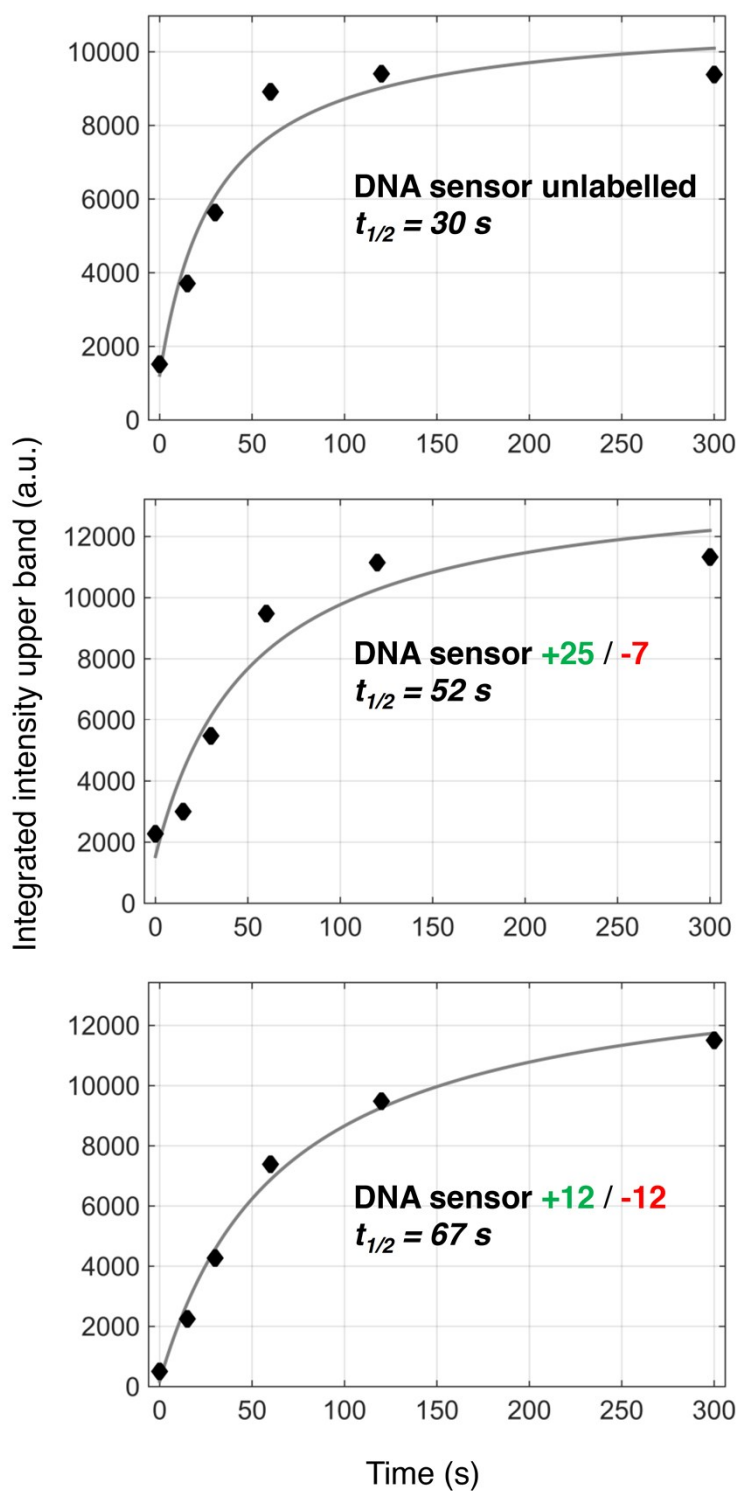


**Figure S9** Polymerization reaction rates determined from band intensities in denaturing polyacrylamide gels. Intensities determined from the non-denatured upper bands in figures S7 and S8 were plotted against time and fitted to Michaelis-Menten kinetics:

$$\text{Intensity upper band} = (\text{maximum intensity} * \text{time}) / (\text{time} + t_{1/2}) + \text{offset}$$

	<b>Sensor +25/-7</b>	<b>Sensor +12/-12</b>
<b>Assay to test completion of synthesis (Figure 2 a+b)</b>	Peak position $\pm 2$ * standard error of fit (= 95% confidence interval)	Peak position $\pm 2$ * standard error of fit (= 95% confidence interval)
DNA	0.676 $\pm$ 0.002	0.514 $\pm$ 0.001
DNA + KF + dNTPs	0.171 $\pm$ 0.002	0.346 $\pm$ 0.002
DNA + PolB + dNTPs	0.175 $\pm$ 0.002	0.361 $\pm$ 0.002
DNA + PolIII $\alpha$ + dNTPs	0.178 $\pm$ 0.003	0.352 $\pm$ 0.002
<b>Binding studies (Figure 3 a+b)</b>		
DNA	0.643 $\pm$ 0.001	0.521 $\pm$ 0.001
DNA + KF	0.661 $\pm$ 0.004 0.884 $\pm$ 0.016	0.521 $\pm$ 0.030 0.620 $\pm$ 0.119
DNA + PolB	0.671 $\pm$ 0.001	0.528 $\pm$ 0.001
DNA + PolIII $\alpha$	0.644 $\pm$ 0.002	0.521 $\pm$ 0.002
<b>Assay to test polymerase pausing (Figure 5 a+b)</b>		
DNA	0.683 $\pm$ 0.002	0.515 $\pm$ 0.001
DNA + KF + dTTPs	0.617 $\pm$ 0.001	0.493 $\pm$ 0.001
DNA + KF + dTTPs + dATPs	0.576 $\pm$ 0.002	0.442 $\pm$ 0.001
DNA + KF + dTTPs + dATPs + dGTPs	0.339 $\pm$ 0.002	0.301 $\pm$ 0.001
DNA + KF + dTTPs + dATPs + dGTPs + dCTPs	0.180 $\pm$ 0.001	0.336 $\pm$ 0.001

**Supplementary Table 1** Peak positions of  $E^*$  histograms that were shown in the main text. The indicated range corresponds to the 95% confidence interval of the Gaussian fit.

Sensor +25/-7	Uncorrected		Corrected for Leakage + Direct Excitation		Corrected for gamma factor (=0.85)		R (nm)
	E*	S	E	S	E	S	
DNA	0.68	0.61	0.65	0.59	0.68	0.50	5.5
DNA + KF + dNTPs	0.17	0.65	0.026	0.62	0.035	0.51	10.8
DNA + POLB + dNTPs	0.18	0.65	0.0053	0.62	0.013	0.51	12.8
DNA + POLIII $\alpha$ + dNTPs	0.18	0.63	0.027	0.61	0.037	0.50	10.7

Sensor +12/-12	Uncorrected		Corrected for Leakage + Direct Excitation		Corrected for gamma factor (=0.72)		R (nm)
	E*	S	E	S	E	S	
DNA	0.51	0.59	0.45	0.56	0.53	0.50	6.1
DNA + KF + dNTPs	0.35	0.62	0.24	0.58	0.30	0.50	7.1
DNA + POLB + dNTPs	0.36	0.60	0.25	0.57	0.32	0.49	7.0
DNA + POLIII $\alpha$ + dNTPs	0.35	0.61	0.24	0.58	0.31	0.50	7.1

Sensor +12/-12	Uncorrected		Corrected for Leakage + Direct Excitation		Corrected for gamma factor (=1.15)		R (nm)
	E*	S	E	S	E	S	
Sensor +25/-7	0.74	0.77	0.72	0.76	0.69	0.50	5.4
Sensor +25/-7, fully extended primer	0.22	0.76	0.04	0.74	0.03	0.49	10.9
Sensor +12/-12	0.56	0.75	0.51	0.74	0.48	0.46	6.3
Sensor +12/-12, fully extended primer	0.39	0.77	0.30	0.74	0.27	0.50	7.3

Supplementary Tables 2, 3 and 4 Raw and corrected values for *E* and *S*. Corrections for leakage and direct excitation were applied, as well as a correction for the gamma factor.